A journal for the publication of
original research in all branches of physics

www.publish.csiro.au/journals/ajp

Phase Transitions and Molecular Reorientations in Bilayered n-Heptadecylammonium Chloride

E. C. Reynhardt

Department of Physics, University of South Africa,
PO Box 392, Pretoria 0003, South Africa.

email: reynhec@alpha.unisa.ac.za

Abstract

An investigation of phase transitions and molecular motions in polycrystalline n-heptadecylammonium chloride ($C_{17}H_{35}NH_3Cl$), employing differential scanning calorimetry, x-ray powder diffraction and nuclear magnetic resonance techniques, is reported. This compound can occur in two virgin polymorphs at room temperature, one interdigitated and one noninterdigitated. The temperature at which crystallisation occurs determines the polymorph that forms. If these polymorphs are heated transitions to noninterdigitated γ, β and α phases occur. Cooling to room temperature shows the same phase transitions, but the virgin phase is not formed. Instead, a noninterdigitated ϵ phase is formed. Defect motions of chain-ends play a significant role in the spin-lattice relaxation rates in all the phases. In the α phase a degree of chain melting is present. The molecular dynamics of chains differs during heating and cooling cycles in the ϵ phase. If the temperature is kept constant during a heating cycle in this phase, fourfold motions of chains are frozen over a period of several hours, but the sample remains noninterdigitated. It seems that the interdigitation process is hampered by the population of defect orientations of chain-ends. The methyl group executes classical threefold reorientations and the NH_3 group jumps in an asymmetric threefold potential well.

1. Introduction

The n-alkylammonium chlorides, with general formula $C_nH_{2n+1}NH_3Cl$ (C_nCl), are bilayered compounds which serve as models for membrane layers (Sackmann 1978; Ringsdorf *et al.* 1988; Hui and Huang 1986; McIntosh *et al.* 1983, 1984; Chapman 1975). From a structural point of view freshly prepared samples of n-alkylammonium chlorides can be divided into three groups. For $10 \leq n \leq 16$ and $1 \leq n \leq 3$ the structures consist of interdigitated aliphatic chains between chlorine layers with the chains N-H$\cdots$Cl hydrogen bonded to the chlorine layers (Kind *et al.* 1982; Schenk *et al.* 1988), as shown in Fig. 1. If a sample which has not been heated above room temperature (virgin sample) is heated, it transforms to noninterdigitated high temperature phases in which the chains tend to be perpendicular to the chlorine layers (Kind *et al.* 1982; Schenk *et al.* 1988, 1989; Seliger *et al.* 1987; Jurga *et al.* 1991; Reynhardt *et al.* 1992; Tsau and Gilson 1968*a*, 1968*b*, 1973; Gilson *et al.* 1976). On cooling, a sample reaches a metastable noninterdigitated ϵ phase (Fig. 1). The transformation to the noninterdigitated state is irreversible (Reynhardt *et al.* 1992). For $4 \leq n \leq 9$ virgin samples are already in a noninterdigitated state and show all the high temperature phases
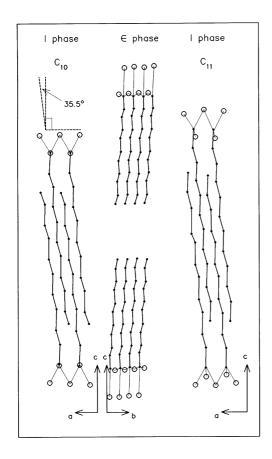
Fig. 1. Orientation of chains in the interdigitated I phase (n even and odd) and the noninterdigitated ϵ phase. Open circles represent chlorine atoms.

on heating and the ϵ phase on cooling. For $n \geq 17$ the virgin phase can be either interdigitated or noninterdigitated. A recent single crystal x-ray diffraction investigation by Scholtz *et al.* (1998) revealed that the virgin phase of $C_{18}Cl$ can crystallise in at least two polymorphs, viz. a noninterdigitated structure, crystallised at room temperature, and an interdigitated structure, crystallised at ~ 276 K. The structure of the noninterdigitated polymorph of $C_{18}Cl$ is illustrated in Fig. 2. The most interesting feature of this structure is the kink in the aliphatic chain at the methylene group adjacent to the ammonium group. It seems that this kink is the result of additional hydrogen bonds between the chlorine atoms and the hydrogen atoms of this methylene group. The structure of the interdigitated phase has not been determined, but most probably it is similar to that of $C_{10}Cl$ (Schenk *et al.* 1989).

The dependence of the long spacing on the number of carbon atoms per chain for a series of C_nCl compounds (Gilson *et al.* 1976; King and Lipscomb 1950; Hughes and Lipscomb 1946; Hendricks 1928*a*, 1928*b*, 1930) is shown in Fig. 3. For the virgin phase (I) the long spacings exhibit two separate linear dependencies on the chain length, viz. one for $1 \leq n \leq 3$ and $10 \leq n \leq 16$ and the other for chains with more than 16 carbon atoms. The long spacing of the noninterdigitated virgin phase of $C_{18}Cl$ (Scholtz *et al.* 1998) coincides with the straight line through the data points for compounds with $n > 16$. Therefore, it is concluded that the
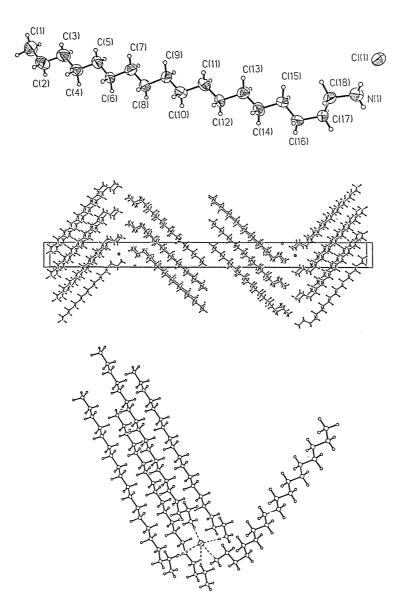
Fig. 2. The packing of chains in the noninterdigitated virgin phase of $C_{18}Cl$ (Scholtz *et al.* 1998). The kink in the chain and the hydrogen bonding between NH_3 hydrogen atoms and neighbouring chlorine atoms are also shown.

noninterdigitated virgin phases of these compounds with $n \geq 17$ have structures similar to that of $C_{18}Cl$ (Scholtz *et al.* 1998). It should be pointed out that the long spacings for $n \geq 17$ published by Gilson *et al.* (1976) have to be multiplied by a factor of two. The values plotted in Fig. 3 have already been corrected.

The structures and molecular dynamics of *n*-alkylammonium chlorides belonging to two of the three groups mentioned above, viz. C_9Cl (Reynhardt and Wozniak-
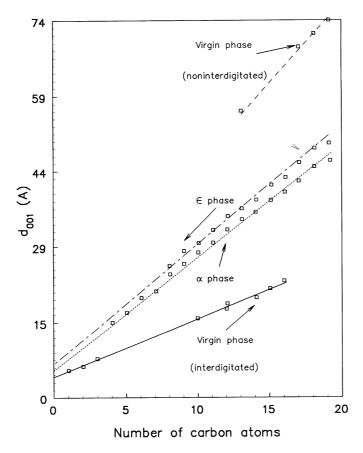
Fig. 3. Dependence of the long spacing in the I, α and ϵ phases as a function of the number of carbon atoms per chain. Data were obtained from papers by Hendricks (1928a, 1928b, 1930), Hughes and Lipscomb (1946), King and Lipscomb (1950), Gilson *et al.* (1976), Reynhardt *et al.* (1992), Reynhardt and Wozniak-Braszak (1993) and Reynhardt (1996).

Braszak 1993), which has a noninterdigitated virgin structure, and $C_{10}Cl$ (Reynhardt *et al.* 1992) and $C_{11}Cl$ (Reynhardt 1996), which have only interdigitated virgin structures, have been reported. With a view to obtaining a full picture of the phase changes and molecular dynamics of n-alkylammonium chlorides, it is necessary to study the polymorphism and molecular dynamics of a polycrystalline sample of an n-alkylammonium chloride with $n \geq 17$ and to compare the results with those of n-alkylammonium chlorides with different virgin structures. In this paper the structural phase transitions and molecular dynamics of $C_{17}Cl$ are reported. Apart from chain reorientations in the noninterdigitated virgin phase, chain-end defect motions and chain disorder in all the phases are described.

2. Experimental

Selectively deuterated polycrystalline samples of n-heptadecylammonium chloride were prepared at the Max-Planck Institut für Polymerforschung in Mainz. One

sample, D3, had partly deuterated NH_3 groups (>80%), while a second sample, C1, was deuterated at the carbon atom adjacent to the NH_3 group. Deuteration of C1 was required for deuteron NMR line-shape experiments which will be done in another laboratory.

All samples for NMR experiments were sealed off in glass ampoules after having been evacuated for several days at $\sim 2 \times 10^{-4}$ Pa. The x-ray camera was evacuated at $\sim 0 \cdot 1$ Pa while diffractograms were recorded. For the DSC experiments an evacuated sample was transfered quickly to the dry nitrogen atmosphere inside the calorimeter. It is well-known that small concentrations of water influence the structures of these compounds. Since the presence of water would complicate the proton NMR results and make a comparison with other similar dehydrated compounds difficult, the abovementioned special precautions were taken.
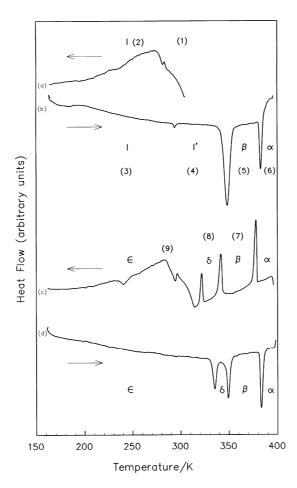

Fig. 4. DSC thermograms of *n*-heptadecylammonium chloride. Arrows indicate changes in temperature while the positions of numbers indicate the temperatures at which x-ray diffractograms were recorded. The different phases, α, β, δ, etc., are discussed in the text.

The instrumentation and experimental methods used in this investigation have been described elsewhere (Fenrych *et al.* 1993*a*, 1993*b*; Jurga *et al.* 1993).

3. Results

(3a) DSC and X-ray Powder Diffraction

The DSC thermograms are shown in Fig. 4. Trace (a) (top) was obtained for a 4·7 mg sample while reducing the temperature from room temperature to 150 K. A broad peak extending from room temperature to ~ 200 K is the main feature of this trace. Trace (b) was obtained while heating the sample from 150 K to 400 K. Three endothermal transitions are observable at 295 K, 349 K and 383 K. The transition at 295 K has a relatively low enthalpy, and depending on the cooling and heating rates, was found to appear within the temperature range 276 K to 300 K. If the cooling rate from room temperature was relatively low, this transition was not observable. An irreversible change in colour of the sample from white to light yellow was observed at the transition at 349 K. Trace (c) shows the transition for a subsequent cooling run from 400 K to 150 K. Three narrow transitions occur at 378 K, 342 K and 322 K. The relatively broad transition between 315 K and 200 K is similar to the one revealed by trace (a). If the same sample is now heated from 150 K to 400 K (trace d), the thermogram differs from the one obtained during the previous heating run (trace b). The weak transition in the vicinity of room temperature is not observable, but a new transition appears at 335 K. The other two transitions are at the same temperatures previously mentioned (trace b). The notation for the different phases (I, I′, δ, β and α), introduced in Fig. 4, will be used in the rest of the discussion.

Table 1.   Interlayer spacings of the different phases of $C_{17}Cl$

Phase	d_{001} (Å)
I	68·96
δ	45·81
β (heating)	42·28
β (cooling)	43·23
α	42·24
ϵ	45·55

X-ray diffractograms, obtained at selected temperatures, are displayed in Fig. 5. The numbers of the diffractograms refer to the numbers in Fig. 4, which indicate the temperatures at which diffractograms were obtained. No noticeable differences could be detected between diffractograms 1 to 4. Although diffractograms 5 to 9 exhibit the same general features, significant differences were observable. Using the same sample, diffractogram 10 was recorded 15 days after diffractogram 9 had been recorded. The long spacings (d_{001}) of the different phases, obtained from the diffractograms shown in Fig. 5, are listed in Table 1. The long spacing of 69·0 Å of the virgin structure (I phase) coincides with the straight line through the data points for noninterdigitated virgin structures in Fig. 3.
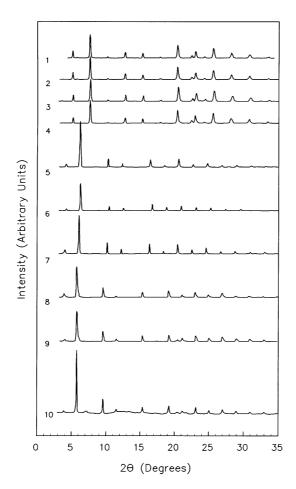
Fig. 5. X-ray diffractograms recorded at different temperatures. Numbers of the diffractograms refer to the temperatures indicated in Fig. 4. Diffractogram 10 was obtained at the same temperature as diffractogram 9, but 15 days later.

(3b) Nuclear Magnetic Resonance

The temperature dependence of M_2 for the virgin C1 and C3 samples heated from $\sim$ 120 K to 400 K is shown in Fig. 6. Cooling sample C1 from the α phase yielded the M_2 values shown as crosses in Fig. 7. The second moments obtained while heating the same sample again from low temperatures are given by squares in the same figure. Leaving sample C1 during a heating cycle at a temperature between 290 K and 350 K for several hours results in an increase in second moment to a value close to that obtained for the same sample in the virgin phase at the corresponding temperature (stars in Fig. 7). Below $\sim$ 270 K M_2 values for sample D3 are $\sim$ 3 G^2 (1 G $\equiv 10^{-4}$ T) lower than for sample C1. The proton spin-lattice relaxation times are shown as a function of inverse temperature for heating from low temperatures in the I phase to the high temperature phases (Fig. 8) and cooling and heating in the ϵ phase (Fig. 9).
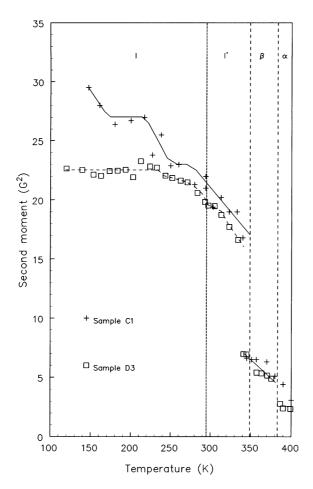
Fig. 6. Proton second moments as a function of temperature. The sample was originally in the noninterdigitated I phase. Vertical dotted lines indicate the approximate temperatures at which phase transitions occur. The other lines serve as a guide to the eye.

4. Discussion and Conclusions

(4a) Nuclear Magnetic Resonance

I and I′ phases. The rigid lattice proton second moment of an $n-$alkane, including intra- and intermolecular dipolar contributions, is given by (Andrew 1950)

$$M_2 = 26 \cdot 3 + \frac{19 \cdot 1}{n+1} \, , \tag{1}$$

where n is the number of carbon atoms per chain. Using this equation and making corrections for the replacement of one methyl group by an ammonium group, good
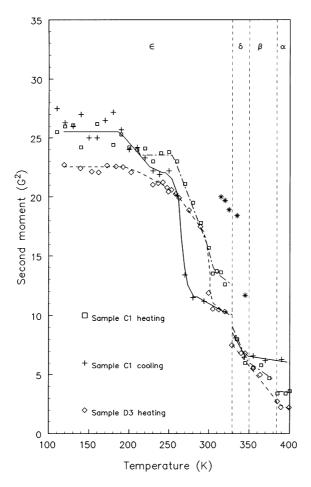
Fig. 7. Proton second moments as a function of temperature. The sample was originally in the noninterdigitated ϵ phase. Vertical dotted lines indicate the approximate temperatures at which phase transitions occur. The other lines serve as a guide to the eye. Stars represent measured values obtained during the heating cycle after the sample had been left at 310 K for 12 hours.

estimates can be obtained for the proton second moments of n-alkylammonium chlorides, including those for chains executing twofold and fourfold reorientations about their long axes. The results are listed in Table 2. The low temperature plateau of 27 ± 2 G^2 for sample C1 (Fig. 6) represents a rigid lattice with reorienting methyl groups, while the second plateau of 23 ± 2 G^2 is in agreement with a rigid lattice and with reorienting CH_3 and NH_3 groups. Since the second moment drops to a value of ~ 18 G^2 in the I' phase, chain reorientations are present in that phase. However, it seems that the reorientation frequency of the latter motion is too low to decrease the second moment to a plateau of ~ 16 G^2, the calculated value for fast twofold reorientations of entire chains, before the transition to the β phase. The plateau of 23 ± 1 G^2 observed between

Table 2.   Calculated proton second moment (in G^2) for molecular reorientations
of the different samples

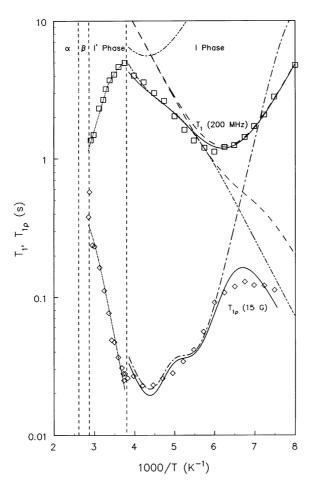| Sample	Rigid	CH_3 C_3	$CH_3 + NH_3$ C_3	Chain C_2	Chain C_4
Cl	28·1	26·7	17	9	
D3	24·8	23·4	—	16	8

Fig. 8.   Proton spin-lattice relaxation times as a function of
inverse temperature in the I phase. Vertical dotted lines indicate
phase transitions. Solid curves represent fits of equations (2),
(3), (5) and (6) to the data. CH_3 reorientation: dashed curve;
NH_3 reorientation: dot–dash curve; and chain-end defect:
dot–dash–dash curve.

170 K and 310 K for sample D3 is in good agreement with the calculated value of
$23·4$ G^2 for a model in which the methyl groups execute threefold reorientations.
Comparison of the M_2 results for the C1 and D3 samples leads to the conclusion
that the M_2 reduction for the former sample between 220 K and 250 K is
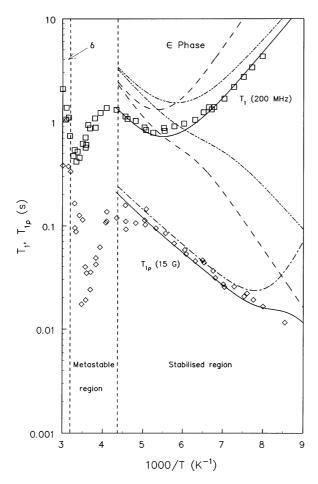definitely due to threefold reorientations of NH_3 groups.

Fig. 9. Proton spin-lattice relaxation times as a function of inverse temperature in the ϵ phase. Vertical dotted lines indicate phase transitions. Solid curves represent fits of equations (2), (3), (5) and (6) to the data below $\beta = 4\cdot3$ K^{-1}. Other curves are the same as in Fig. 8.

If it is assumed that the rate of transfer of spin energy between nuclei is faster than the rate of transfer of energy to the lattice, the relaxation rates due to the modulation of dipolar interactions are given by (Kubo and Tomita 1954)

$$\frac{1}{T_1} = \tfrac{2}{3}\gamma_H^2 \sum_i \Delta M_{2i}\left(\frac{\tau_{ci}}{1+\tau_{ci}^2\omega_0^2} + \frac{4\tau_{ci}}{1+4\tau_{ci}^2\omega_0^2}\right), \tag{2}$$

$$\frac{1}{T_{1\rho}} = \gamma_H^2 \sum_i \Delta M_{2i}\frac{\tau_{ci}}{1+4\tau_{ci}^2\omega_1^2}, \tag{3}$$

where

$$\tau_{ci} = \tau_{0i}\exp(E_i/RT) \tag{4}$$

and ω_0 and $H_1 = \omega_1/\gamma_H$ are the Larmor frequency and the spin locking field, respectively. Here ΔM_{2i} is the second moment reduction due to molecular reorientaion i. Considering only threefold reorientations of methyl ($i = 1$) and NH$_3$ groups ($i = 2$), it is not possible to obtain an acceptable simultaneous fit to the T_1 and $T_{1\rho}$ data with E_i, τ_{0i} and ΔM_{2i} as variable parameters for both methyl and NH$_3$ group reorientations, if the ΔM_2 values are kept in reasonable agreement with the calculated proton second moment reductions of $1 \cdot 4$ G^2 and $2 \cdot 0$ G^2, respectively. A similar problem was encountered in the case of C$_{10}$Cl and the only model which gave agreement with the data was one in which the NH$_3$ group reorients in a potential well with three unequal minima (Reynhardt *et al.* 1992). This model is realistic if the nonequivalent hydrogen bonds between hydrogen atoms of the ammonium group and neighbouring chlorines are kept in mind (Scholtz *et al.* 1998). Polak and Ailion (1977) and Latanowicz and Pajak (1989) derived expressions for the relaxation rates due to reorientations in a potential well with three unequal minima, viz:

$$\frac{1}{T_1} = \gamma_H^2 \Delta M_2 \left\{ \frac{3a_1}{(a_1 + 2)^2} \left(\frac{\tau_1}{1 + \omega_0^2 \tau_1^2} + \frac{4\tau_1}{1 + 4\omega_0^2 \tau_1^2} \right) \right.$$
$$\left. + \frac{1}{(a_2 + 2)} \left(\frac{\tau_2}{1 + \omega_0^2 \tau_2^2} + \frac{4\tau_2}{1 + 4\omega_0^2 \tau_2^2} \right) \right\}, \qquad (5)$$

$$\frac{1}{T_{1\rho}} = \tfrac{3}{2}\gamma_H^2 \Delta M_2 \left\{ \frac{3a_1}{(a_1 + 2)^2} \left(\frac{\tau_1}{1 + \omega_1^2 \tau_1^2} \right) + \frac{1}{(a_2 + 2)} \left(\frac{\tau_2}{1 + 4\omega_1^2 \tau_2^2} \right) \right\}, \qquad (6)$$

where

$$\tau_j = \tau_{0j} \exp \frac{E_j}{RT}$$

$$a_j = \exp \frac{\Delta E_j}{RT} . \qquad (7)$$

The energies E_j and ΔE_j have been defined (Reynhardt *et al.* 1992). A reasonable fit of equations (2), (3) (for CH$_3$ groups), (5) and (6) (for NH$_3$ groups) to both sets of data was obtained with the parameters listed in Table 3. However, it was clear that, apart from the CH$_3$ and NH$_3$ reorientations, an additional mechanism is effective in influencing both T_1 and $T_{1\rho}$. In the case of T_1 this mechanism plays a noticeable role in the region just below the transition from the I phase to the I$'$ phase, while it seems to influence $T_{1\rho}$ at the lowest temperatures.

It is assumed that chain-end defect motions also contribute to the relaxation rates in the I and I$'$ phases (Basson and Reynhardt 1990). Andrew and Latanowicz (1968) derived relaxation rate equations for the jumping of a proton between two equilibrium sites with unequal energy. In principle this model could also be applied to defect motions of chains (Fenrych *et al.* 1993*a*, 1993*b*; Jurga *et al.*

1993; Basson and Reynhardt 1990, 1991, 1992), but in the present situation the overlapping of more effective relaxation mechanisms with the chain-end defect motions makes the isolation of all these parameters impossible. However, with a view to obtaining a rough estimate of the contribution of defect motions to the relaxation rates in the I phase, it was assumed that the populations of defect and all-trans orientations are equal (fast reorientations between all-trans and defect orientations). The parameters listed in Table 3 were thus obtained. The second moment reduction of $\sim 0 \cdot 3$ G^2 is much smaller than the second moment reductions associated with the threefold reorientations of NH$_3$ and methyl groups, but is in agreement with reductions obtained for other compounds in which defect motions could be studied successfully (Basson and Reynhardt 1990, 1991, 1992). The best fit to the data, shown as solid curves in Fig. 9, includes the contributions from three reorientation mechanisms, viz. threefold reorientations of CH$_3$ and NH$_3$ groups and a defect motion of chain-ends. The temperature dependence of T_1 and $T_{1\rho}$ in the noninterdigitated I phase of C$_{17}$Cl is similar to that in the interdigitated I phase of C$_{10}$Cl (Reynhardt *et al.* 1992).

Table 3. Motional parameters obtained from fits to the relaxation results

Motion	Parameter	I phase	I′ phase	ϵ phase
NH$_3$ C$_3$	E_1 (kJ/mol)	23±2		10·9±1·0
	E_2 (kJ/mol)	18±2		10·9±1·0
	ΔE_1 (kJ/mol)	8·4±1·0		5·0±0·5
	E_2 (kJ/mol)	5·9±1·0		5·0±0·5
	$\log[\tau_{01}$ (s)]	−11·2±0·2		−10·5±1·0
	$\log[\tau_{02}$ (s)]	−11·2±0·2		−10·5±1·0
	ΔM_2 (G^2)	1·9±0·2		2·0±0·2
CH$_3$ C$_3$	E (kJ/mol)	10·5±1·0		10·9±0·5
	$\log[\tau_0$ (s)]	−12·7±0·1		−12·3±0·2
	ΔM_2 (G^2)	1·5±0·2		1·4±0·2
Defect motion	E (kJ/mol)	11·3±1·0		8·4±2·0
	$\log[\tau_0$ (s)]	−11·8±1·0		−11·8±1·0
	ΔM_2 (G^2)	0·3±0·1		1·2±0·5
Chain motion			29±3	

ϵ *phase.* The proton second moment for sample C1 (crosses in Fig. 7) just below the $\delta \to \epsilon$ transition temperature during a cooling cycle is ~ 10 G^2, which is in agreement with the calculated value for fourfold reorientations of chains. The sharp increase in M_2 between 280 K and 250 K to ~ 22 G^2, therefore, reveals the freezing of fourfold reorientations of entire chains. The plateau of $\sim 22 \cdot 5$ G^2 in the vicinity of 240 K is in reasonable agreement with the calculated value of $24 \cdot 7$ G^2 for stationary chains and CH$_3$ and NH$_3$ groups executing threefold reorientations. The discrepancy between calculated and measured values can be accounted for in terms of chain defect motions. The plateau of ~ 26 G^2 at lower temperatures agrees well with the calculated value for a rigid lattice with reorienting methyl groups.

During a heating cycle the second moment below 210 K is the same as during the cooling run. However, if the temperature is increased above ~ 210 K, the

second moment deviates from that obtained during the cooling cycle. Both the plateaus in the vicinity of 240 K and 315 K are ~ 2 G^2 higher than the corresponding ones observed during the cooling cycle. Another interesting aspect of the M_2 data between 260 K and 350 K is that it is time dependent. These observations point to the existence of a metastable state. It is concluded that the fourfold reorientations of chains, which were identified during the cooling cycle, are also activated during the heating cycle, but become frozen as a function of time. It is emphasised that although the second moment values approach those observed in the virgin sample after a period of hours, the structure does not become interdigitated. The x-ray diffractogram obtained 15 days after the sample had been heated to the α phase, shows unambiguously that the sample is still noninterdigitated (Fig. 5).

The metastable region of the ϵ phase ($3 \cdot 4 < \beta < 5 \cdot 0$ K^{-1}) is indicated in Fig. 9. The shallow H_1 independent $T_{1\rho}$ minimum at $\beta \simeq 4 \cdot 5$ K^{-1} falls within this region and corresponds to a second moment reduction which is far too small to account for any reorientation involving entire chains. It seems that the gradual change in structure results in an anomalous behaviour of $T_{1\rho}$ as a function of temperature in the metastable region. The decrease in $T_{1\rho}$ for $\beta > 5$ K^{-1} corresponds to the final increase in M_2 below 220 K and is, like in the case of the I phase, associated mainly with threefold reorientations of NH$_3$ groups. However, it was not possible to obtain an acceptable fit to both the T_1 and $T_{1\rho}$ relaxation data without introducing a contribution from defect motions. Since the $T_{1\rho}$ values did not reach a minimum, it was not possible to obtain detailed information about the defect motion and the NH$_3$ reorientation. The fit shown as solid curves in Fig. 9 was obtained with the parameters listed in Table 3. However, it should be kept in mind that these parameters are relatively inaccurate. The fact that the activation energy for the threefold reorientation of the NH$_3$ group in the ϵ phase is much lower than in the I phase, is an indication that hydrogen bonding between NH$_3$ hydrogen atoms and chlorine atoms is weaker in the ϵ phase. In this phase the defect reorientations of chain-ends make a significant contribution to T_1, but the effect on $T_{1\rho}$ is negligible.

High temperature phases. The measured second moment value of ~ 7 G^2 in the β phase during a heating cycle suggests that the chains execute fourfold reorientations in this phase. However, the fact that this value is somewhat lower than the calculated value of 9 G^2 and is further reduced to ~ 5 G^2 with increasing temperature is a clear indication that defect motions are present in this phase. The further reduction to ~ 3 G^2 in the α phase is due to the superposition of further defect motions on the chain reorientations, which can be described as the partial melting of the noninterdigitated chains. These conclusions are supported by the x-ray results (Section 4*b*), which show that the length of the c axis is too short to accommodate fully stretched chains.

During the cooling cycle second moment values of sample C1 in the high temperature α and β phases are higher than those observed during the heating cycle at corresponding temperatures. The value of ~ 6 G^2 indicates that defect motions are present, but that the population of defect orientations is less than during the cooling cycle. In Section 4*b* this result will be linked to the observation that the c cell-dimension is larger in the β (cooling) phase than in the β (heating) phase.

(4b) Thermal Analysis and X-ray Diffraction

I and I′ phases. From the discussion of the NMR results (Section 4a) it is known that the chains execute fourfold reorientations in the I′ phase. However, since hydrogen bonding between NH_3 groups and chlorine atoms is expected to be fairly strong, it is unlikely that the potential well in which the chains execute the fourfold reorientations is symmetric. Therefore, it is possible that the structure of the organic layer is motionally disordered in the I′ phase. If the sample is cooled down slowly, the disorder is removed from the structure and the ordered I phase is reached. The weak DSC transition is associated with this process. However, if the sample is cooled down fast from the I′ phase, some of the defect chain orientations are frozen in and the I phase differs from the original one. If the temperature is now increased, the transition from the I to the I′ phase occurs at a different temperature, as observed in the DSC thermograms. Investigations of similar compounds (Fenrych *et al.* 1993a; Jurga *et al.* 1993; Zuniga and Chapuis 1985) have shown that static defects of chains are present in the I phase, but absent in the I′ phase. Due to chain packing effects the energy of the defect orientation is lower than that of the all-transorientation in the I phase.

High temperature noninterdigitated α, β and δ phases. The transition at 349 K (trace (c) in Fig. 4) results in an orthorhombic β phase and the one at 383 K in a tetragonal α phase (Tsau and Gilson 1968; Gilson *et al.* 1976). In the α phase the chains are oriented with their long axes parallel to the crystallographic c axis. The first transition results in a dramatic increase of the c cell-dimension to $\sim 42 \cdot 5$ Å, in agreement with the result reported by Gilson *et al.* (1976). This long spacing is not adequate to accommodate a fully noninterdigitated structure with chains in the all-trans configuration. Excluding the chlorine layer, a minimum distance of 43 Å is required to accommodate fully stretched noninterdigitated chains. Therefore, it is concluded that chain-end defects (Reynhardt *et al.* 1992) decrease the effective length of the chains in the α and β phases. From NMR studies of bilayered compounds, it is known that defect motions of chain-ends are present in the high temperature phases (Jurga *et al.* 1991, 1993; Basson and Reynhardt 1990; Fenrych *et al.* 1993a, 1993b). In some cases defect orientations along the chains are populated to such an extent in the α phase that the term 'chain melting' is used (Fenrych *et al.* 1993a, 1993b; Fernandez *et al.* 1982; Kind *et al.* 1979). From the second moment results (Section 4a) it is clear that the chains have a very high degree of mobility in the α phase. It is therefore concluded that defects are the main cause of the shorter c axis. If the sample is cooled from the α to the β phase (trace (c) in Fig. 4), the length of the c axis is ~ 1 Å longer than in the β (heating) phase. The observed elongation corresponds to $\Delta 2\theta \simeq 0 \cdot 1°$, which is significant. A similar effect was observed by Gordon and Stenhagen (1953) in $C_{12}Cl$. As revealed by the second moment results, this elongation is due to a lower population of defect orientations of chains in the β (cooling) phase than in the β (heating) phase, implying that the transition from the α to the β phase is not purely of the first order (Rao and Rao 1978). The δ phase (trace c) was not observed during the heating run (trace b). The c axis of this noninterdigitated phase is $\sim 6\%$ longer than in the β phase. This increase in the c cell-dimension is due to the elimination of some of the kink defects which are present in the β phase. Once again, this conclusion is supported by the second moment results.
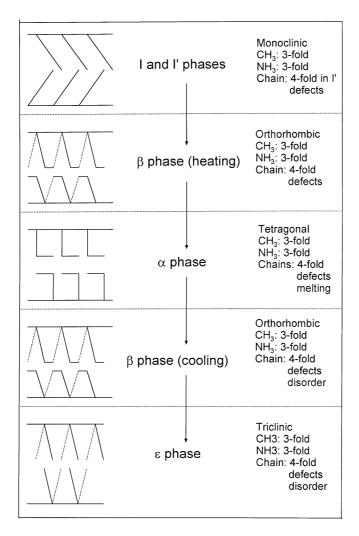
Fig. 10. Representation of chain orientations and reorientations in the different phases of $C_{17}Cl$. Pairs of adjacent parallel horizontal lines represent layers of chlorine atoms. Lines inclined to or perpendicular to these layers are $n-C_{17}H_{35}$ chains. Broken lines indicate alternative orientations of the chains, e.g. in fourfold reorientations. Short horizontal lines at chain-ends represent defect orientations. The length of such a line is an indication of the population of defect orientations in a specific phase.

Noninterdigitated ϵ phase. The c cell-dimension of this noninterdigitated phase is almost the same as that of the δ phase. The chains are tilted with respect to the normal to the inorganic layer (Fig. 1). The presence of chain-end defects, which have been shown by the NMR results to be dynamic, is implied. From Fig. 3 it is clear that the length of the long axis of C_nCl compounds in the noninterdigitated ϵ phase is also linearly dependent on the number of carbon atoms per chain.

(4c) Chain Orientations and Reorientations

If hydrogen bonds between NH_3 protons and chlorine atoms are weak, the chains reorient about their long axes, but if these bonds are strong, the chains are forced to reorient about the C–N bonds. The potential barrier to such a chain reorientation is obviously much higher than the barrier to a reorientation about the long axis. In the β and α phases hydrogen bonds between NH_3 groups and neighbouring chlorine atoms are relatively weak (Schenk *et al.* 1989) and the chain axes tend to be parallel to the normal to the bilayer (Jurga *et al.* 1991). In these phases the chains reorient about their long axes. In the ϵ phase a hydrogen bond network starts to form and chain defect populations are lower. In $C_{10}Cl$ the chains are tilted with respect to the normal to the chlorine layer in this phase. The packing of the chains is less dense than in the I phase and they execute fourfold reorientations. However, the four potential wells are not of equal depth, resulting in unequal occupation of the different orientations (Jurga *et al.* 1991). At room temperature the structure is therefore orientationally disordered. It is clear that a fairly large area per chain is required in the *ab* plane to accommodate the disorder and the chain reorientations about the C–N bonds. As the temperature is decreased, some of the orientations of the chains become less populated and the *a* and *b* cell-dimensions decrease drastically (Reynhardt *et al.* 1992), resulting in a denser packing of chains with a higher activation energy for chain reorientations. Below 210 K the structure is fairly ordered and the packing of the chains is much denser than at room temperature. The broad DSC transition revealed by trace (c) in Fig. 4 is associated with this process. The orientations and dynamics of chains in the different phases of $C_{17}Cl$ are illustrated in Fig. 10.

An increase in temperature above 210 K starts a process which tends to interdigitate the structure, but the presence of defects hampers the process. It is clear that the activation energy of chain reorientations will be increased. Fourfold reorientations are, therefore, frozen within a relatively short time. The x-ray results show that after 15 days the compound has not returned to a partly interdigitated structure. In $C_{10}Cl$ a very small but significant reduction in the length of the *c* cell-dimension in the ϵ phase was observed while heating the sample (Reynhardt *et al.* 1992).

(4d) Comparison with Other n-alkylammonium Chlorides

The main difference between $C_{17}Cl$ and the other *n*-alkylammonium chlorides is the structure of the noninterdigitated virgin polymorph. The hydrogen bonding between the hydrogen atoms of one of the methylene groups and chlorine atoms, resulting in a chain defect next to the ammonium group, has not been observed in *n*-alkylammonium chlorides. It seems that this defect in the chain could prevent the interdigitation of chains. Although this structure is noninterdigitated, its molecular dynamics is similar to that of the interdigitated virgin structures of $C_{10}Cl$ (Reynhardt *et al.* 1992) and $C_{11}Cl$ (Reynhardt 1996), implying that the chain packing is as dense in the noninterdigitated $C_{17}Cl$ virgin structure as in the interdigitated virgin structures of the other compounds. After the transition to any of the high temperature noninterdigitated phases, the phase behaviour and molecular dynamics of $C_{17}Cl$ are similar to those of the other

compounds in the family. It is known that n-alkylammonium chlorides do not convert back to the interdigitated virgin phase after heating to one of the high temperature phases (Reynhardt *et al*. 1992). The results of the present study have shown that, although the virgin phases of compounds with $n \geq 17$ are noninterdigitated, they do not transform back to that structure after heating to one of the high temperature phases. Instead, they transform to the noninterdigitated ϵ phase, like all the other n-alkylammonium chlorides.

Acknowledgments

References

Andrew, E. R. (1950). *J. Chem. Phys.* **18**, 607.
Andrew, E. R., and Latanowicz, L. (1986). *J. Magn. Reson.* **68**, 232.
Basson, I., and Reynhardt, E. C. (1990). *J. Chem. Phys.* **93**, 3604.
Basson, I., and Reynhardt, E. C. (1991). *J. Chem. Phys.* **95**, 1215.
Basson, I., and Reynhardt, E. C. (1992). *J. Chem. Phys.* **97**, 1287.
Chapman, D. (1975). *Quart. Rev. Biophys.* **8**, 185.
Fenrych, J., Reynhardt, E. C., Jurga, S., and Jurga, K. (1993*a*). *Mol. Phys.* **78**, 1117.
Fenrych, J., Reynhardt, E. C., Jurga, S., and Jurga, K. (1993*b*). *Mol. Phys.* **79**, 559.
Fernandez, J., Socias, C., Arriandiaga, M. A., Tello, M. J., and Echarri, A. L. (1982). *J. Phys.* C **15**, 1151.
Gilson, D. F. R., Kertes, A. S., Manley, R. St. J., and Tsau, J. (1976). *Can. J. Chem.* **54**, 765.
Gordon, M., and Stenhagen, E. (1953). *Acta Crystallogr.* **6**, 739.
Hendricks, S. B. (1928*a*). *Z. Kristallogr.* **67**, 119.
Hendricks, S. B. (1928*b*). *Z. Kristallogr.* **68**, 189.
Hendricks, S. B. (1930). *Z. Kristallogr.* **74**, 29.
Hughes, E. W., and Lipscomb, W. N. (1946). *J. Am. Chem. Soc.* **68**, 1970.
Hui, S. W., and Huang, C. (1986). *Biochemistry* **25**, 1330.
Kind, R., Plesko, S., Arend, H., Blinc, R., Zeks, B., Seliger, J., Lozar, V., Lahajnar, G., Milia, F., and Chapuis, G. (1979). *J. Chem. Phys.* **71**, 2118.
Kind, R., Blinc, R., Muralt, P., Slak, J., Chapuis, G., and Schenk, K. J. (1982). *Phys. Rev.* **26**, 1816.
King, M. V., and Lipscomb, W. N. (1950). *Acta Crystallogr.* **3**, 222.
Kubo, R., and Tomita, K. (1954). *J. Phys. Soc. Jpn* **9**, 888.
Jurga, S., Macho, V., Húser, B., and Spiess, H. W. (1991). *Z. Phys.* B **84**, 43.
Jurga, S., Jurga, K., Reynhardt, E. C., and Katowski, P. (1993). *Z. Naturforsch.* **48a**, 563.
Latanowicz, L., and Pajak, Z. (1989). *Ber. Bunsenges. Phys. Chem.* **93**, 440.
McIntosh, T. J., McDaniel, R. V., and Simon, S. A. (1983). *Biochim. Biophys. Acta* **731**, 109.
McIntosh, T. J., Simon, S. A., Ellington, J. C., and Porter, N. A. (1984). *Biochemistry* **23**, 4038.
Polak, M., and Ailion, D. C. (1977). *J. Chem. Phys.* **67**, 3029.
Rao, C. N. R., and Rao, K. J. (1978). *In* 'Phase Transitions in Solids', Chap. 2 (McGraw–Hill: New York).
Reynhardt, E. C. (1996). *Chem. Phys. Lett.* **256**, 548.
Reynhardt, E. C., and Wozniak-Braszak, A. (1993). *Chem. Phys. Lett.* **215**, 493.
Reynhardt, E. C., Jurga, S., and Jurga, K. (1992). *Mol. Phys.* **77**, 257.
Ringsdorf, H., Schlarb, B., and Venzmer, J. (1988). *J. Angew. Chem.* **100**, 117.
Sackmann, E. (1978). *Ber. Bunsenges. Phys. Chem.* **82**, 891.
Schenk, K. J., Chapuis, G., Kind, R., and Seliger, J. (1988). *J. Molec. Struct.* **176**, 331.

Schenk, K. J., Ogle, C. A., Chapuis, G., Cavagnat, R., Jokic, A., and Rey-Lafon, M. (1989). *J. Phys. Chem.* **93**, 5040.

Scholtz, R., Reynhardt, E. C., and Kruger, G. J. (1998). Polymorphism in the bilayered compound *n*-octadecylammonium chloride. *J. Solid State Chem.*, submitted.

Seliger, J., Zagar, V., Blinc, R., Kind, R., Arend, H., Chapuis, G., Schenk, K. J., and Milia, F. (1987). *Z. Phys.* B **69**, 379.

Tsau, J., and Gilson, D. F. R. (1968*a*). *J. Phys. Chem.* **72**, 4082.

Tsau, J., and Gilson, D. F. R. (1968*b*). *Can. J. Chem.* **52**, 2421.

Tsau, J., and Gilson, D. F. R. (1973). *Can. J. Chem.* **51**, 1990.

Zuniga, F. J., and Chapuis, G. (1985). *Mol. Cryst. Liq.* **128**, 349.